ANTICANCER RESEARCH *40*: 4675-4680 (2020)
doi:10.21873/anticanres.14466

Effect of Isomerization of TX-2036 Derivatives on the Interaction With Tyrosine Kinase Domain of EGF Receptor

KAZUTO OHKURA[1], ATSUSHI TABATA[2], YOSHIHIRO UTO[2] and HITOSHI HORI[2]

[1]*Graduate School of Pharmaceutical Sciences, Suzuka University of Medical Science, Suzuka, Japan;*
[2]*Department of Biological Science and Technology, Life System, Institute of Technology and Science, The University of Tokushima Graduate School, Tokushima, Japan*

Abstract. *Background: From the design and synthesis of enantiomers, we can expect to obtain two compounds with different pharmacokinetics and pharmacological activities at the same time, which is thought to lead to the development of efficient anticancer agents. Chiral-2-nitroimidazole TX-2036 derivatives exhibit stereo-configuration (R- and S-configuration)-dependent tyrosine kinase inhibitory activity, and the activity of the tyrosine kinase domain of EGF receptor (EGFR-tyk) is suppressed. In order to clarify the reason why the effects on EGFR-tyk activity differ depending on stereoisomers, we tried to analyze the interaction between each TX-2036 derivative and EGFR-tyk. Materials and Methods: The 2-nitroimidazole-based radiosensitizer TX-2036 series were synthesized and their molecular features were examined using protein kinase inhibition assay and molecular structural analysis. Results: R-configured TXs (TX-2043, -2030, and -2036) exhibited more potent protein kinase inhibitory activity than S-configured TXs (TX-2044, -2031, and -2037), and the IC_{50} value of TX-2036 was 1.8 μM. Conclusion: R-configured TXs interacted with Lys^{721} and Thr^{766} of EGFR-tyk. The combinations of amino acid residues targeted by the S-configured TXs were different from each other (Ile^{765} and Thr^{766} (TX-2044), Ser^{696}, Thr^{766}, and Thr^{830} (TX-2031), Gly^{772}, Cys^{773}, and Thr^{830} (TX-2037)). Preparing a series of isomers with different target sites was considered beneficial when the target was mutated.*

We previously reported on the molecular design and evaluation of enantiomerically pure chiral haloacetylcarbamoyl-2-nitroimidazoles (TX-1898 series), including chloro- and bromo-derivatives, as antiangiogenic hypoxic cell radiosensitizers (1). Softer nucleophiles, such as non-protein thiols and thiol proteases, are present in the tumor microenvironment. Therefore, we designed the 2-nitroimidazole derivatives that incorporate a softer electrophile, the aminomethylenecyclopentenedione moiety, as the antiangiogenic and antitumor functional group. The effect of the molecular chirality and side chain bulkiness of the designed 2-nitroimidazole derivatives on biological activities have already been examined (2). Two potential benefits of a chiral center in our hypoxic cell radiosensitizers are as follows: enantiomers provide two molecular structures expected to exhibit different biological activities from the same synthetic route and each enantiomer exhibits specific pharmacokinetic and pharmacodynamic properties. Moreover, 2-nitroimidazole-based antiangiogenic hypoxic cell radiosensitizers (TX-2036 series) that incorporate the 2-aminomethylene-4-cyclopentene-1,3-dione moiety have been designed (3). The radiation-sensitizing ability of TX-2036 derivatives were previously sown to be influenced by the structure of the chiral-2-nitroimidazole region (4). TX-2036 derivatives exhibited protein kinase (*e.g.* EGF receptor (EGFR)-involved tyrosine kinase domain) inhibition, and *R*-configured derivatives showed more potent inhibitory activity than *S*-configured derivatives. In the present study, interactive analyses were performed between TX-2036 derivatives and the tyrosine kinase domain of EGFR (EGFR-tyk).

Correspondence to: Prof. Kazuto Ohkura, Graduate School of Pharmaceutical Sciences, Suzuka University of Medical Science, 3500-3 Minamitamagaki-cho, Suzuka, Mie 513-8670, Japan. Tel: +81 593400611, Fax: +81 593681271, e-mail: kohkura@suzuka-u.ac.jp

Key Words: Molecular design, structure, EGF receptor, TX-2036 derivatives.

Materials and Methods

Assay for EGFR involved tyrosine kinase activity. A431 human epithelial carcinoma cells were solubilized and cell debris were removed. The cell lysate was incubated with or without EGF at 25˚C for 30 min, and the reaction was initiated by the addition of [γ-^{32}P]ATP and incubated at 0˚C for 10 min. After the reaction was stopped, the mixture was washed. The phosphorylation of EGFR was estimated as ^{32}P radioactivity using a scintillation counter (3, 5).

Interactive analysis between TX-2036 derivatives and EGFR-tyk. X-ray data of the protein kinase domain of EGFR were obtained from the Protein Data Bank (ID=1M17). TX-2036 derivatives were synthesized as previously described (3), and conformation analyses were performed using CAChe-Conflex (Fujitsu Inc., Japan) (6, 7).

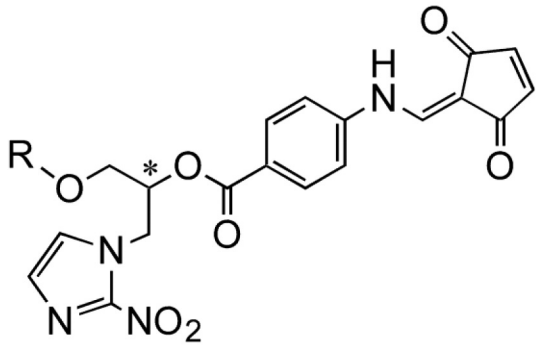

1. TX-2043: *R*-configuration, R=methyl
2. TX-2044: *S*-configuration, R=methyl
3. TX-2030: *R*-configuration, R=*tert*-butyl
4. TX-2031: *S*-configuration, R=*tert*-butyl
5. TX-2036: *R*-configuration, R=*p-tert*-butyl
6. TX-2037: *S*-configuration, R=*p-tert*-butyl

Figure 1. *Structure of TX-2036 derivatives.*

Figure 2. *Cavity analysis of EGFR-tyk. The ligand-bindable pockets (dark gray clouds) of protein kinase domain of EGFR were examined using the Molegro Virtual Docker.*

An interactive analysis of TX-2036 derivatives with the protein kinase domain of EGFR was performed using Molegro Virtual Docker (CLC bio., Aarhus, Denmark) as preciously described (8, 9). The ligand-bindable pockets of the protein kinase domain of EGFR were examined using the Molegro Virtual Docker (CLC bio., Aarhus, Denmark).

Results

Tyrosine kinase inhibitory activities of TX-2036 derivatives. The structures of TX-2036 derivatives are shown in Figure 1. These compounds had a chiral center, and were classified into the *R*-configuration (TX-2043, -2030, and -2036) and *S*-configuration (TX-2044, -2031, and -2037). In methyl group-containing derivatives, *R*-configured TX-2043 inhibited EGFR-tyk activity and the IC_{50} value was 2.3 μM (Table I). The EGFR-tyk inhibition of *S*-configured TX-2044 was weaker than that of TX-2043, and the IC_{50} value was 23.0 μM. TX-2030 (*tert*-butyl containing *R*-configured) more strongly inhibited EGFR-tyk (IC_{50}=21.3 μM) than TX-2031 (*tert*-butyl containing *S*-configured) (IC_{50}=213.0 μM). The EGFR-tyk inhibition of *p-tert*-butyl containing TX-2036 (R-configured, IC_{50}=1.8 μM) was stronger than that of TX-2037 (*S*-configured, IC_{50}=18.4 μM).

Table I. *Effect of TX-2036 derivatives on tyrosine kinase activities.*

TXs (chirality)	IC_{50} (μM)
TX-2043 (R)	2.3
TX-2044 (S)	23.0
TX-2030 (R)	21.3
TX-2031 (S)	213.0
TX-2036 (R)	1.8
TX-2037 (S)	18.4

Values of IC_{50} (μM) were summarized from (3).

Interaction between TX-2036 derivatives and tyrosine kinase domain of EGFR. The tyrosine kinase domain of EGFR (1M17) had ligand-bindable sites (dark gray clouds in Figure 2). TX-2043 became trapped in the ligand bindable site of EGFR-tyk, and interacted with Lys^{721} and Thr^{766} by the 2-nitroimidazole region (Figures 3 and 4) (Table II). TX-2044 interacted with EGFR-tyk as well as TX-2043 (Figure 3), whereas TX-2044 acted on different amino acid residues (Ile^{765} and Thr^{766}) from TX-2043 (Figure 4). The *tert*-butyl containing TX-2030 interacted with Lys^{721} and Thr^{766} by the 2-nitroimidazole region. The target amino acid residues of TX-2031 differed from those of TX-2030, and TX-2031 interacted with Ser^{696}, Thr^{766}, and Thr^{830}. TX-2036 interacted with Lys^{721} and Thr^{766} of EGFR-tyk as well as TX-2043 and TX-2030. TX-2037 interacted with different amino acid residues from TX-2036, and acted on Gly^{772}, Cys^{773}, and Thr^{830}. *R*-configured TX-2036 derivatives (TX-2043, -2030, and -2036) interacted with the same amino acid residues (Lys^{721} and Thr^{766}), whereas *S*-configured derivatives (TX-2044, -2031, 2037) interacted various different amino acids of EGFR-tyk.

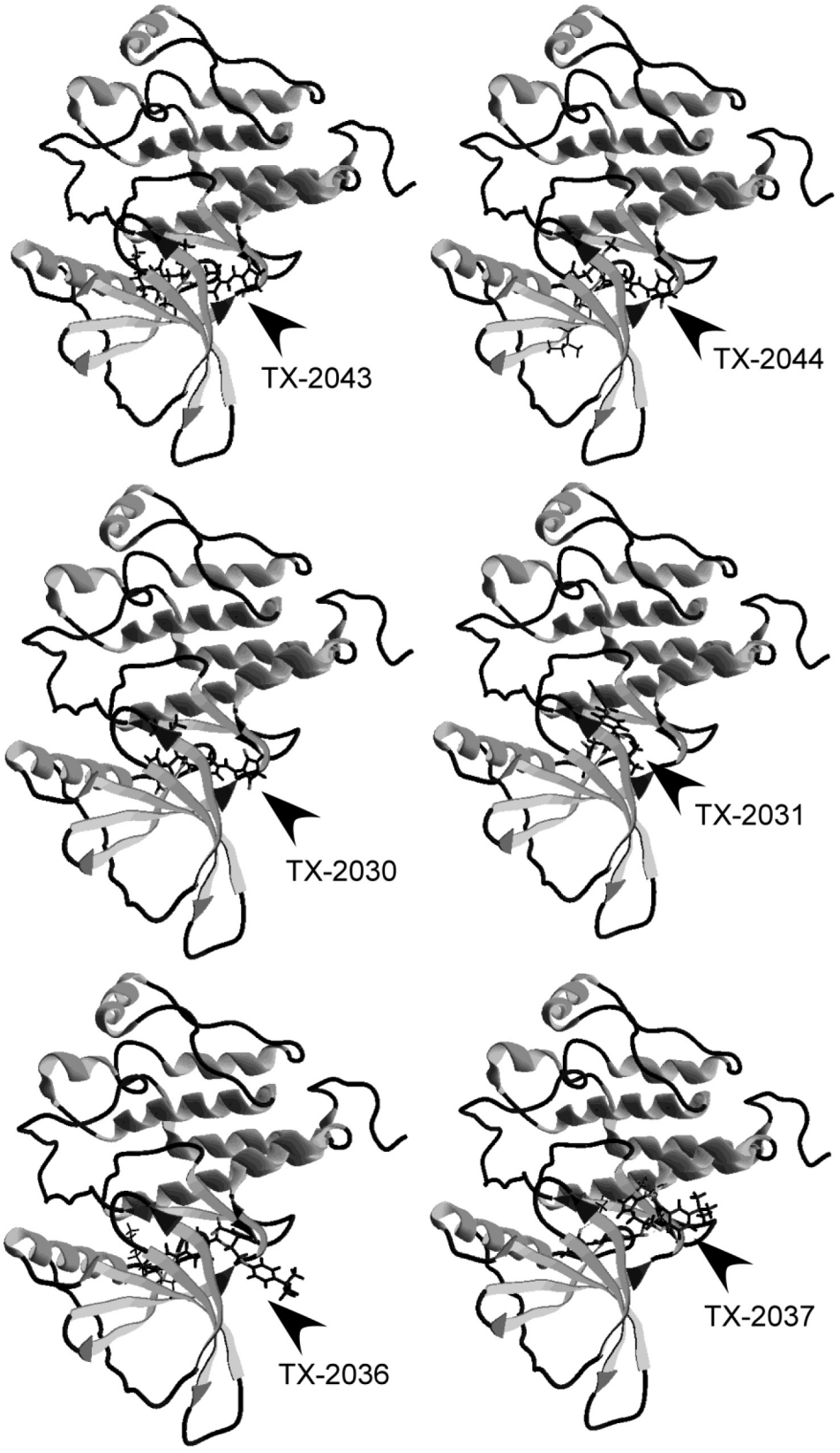

Figure 3. *Interactive analysis of TX-2036 derivatives with EGFR-tyk. TX-2036 derivatives fitted into the cavity of the EGFR-tyk.*

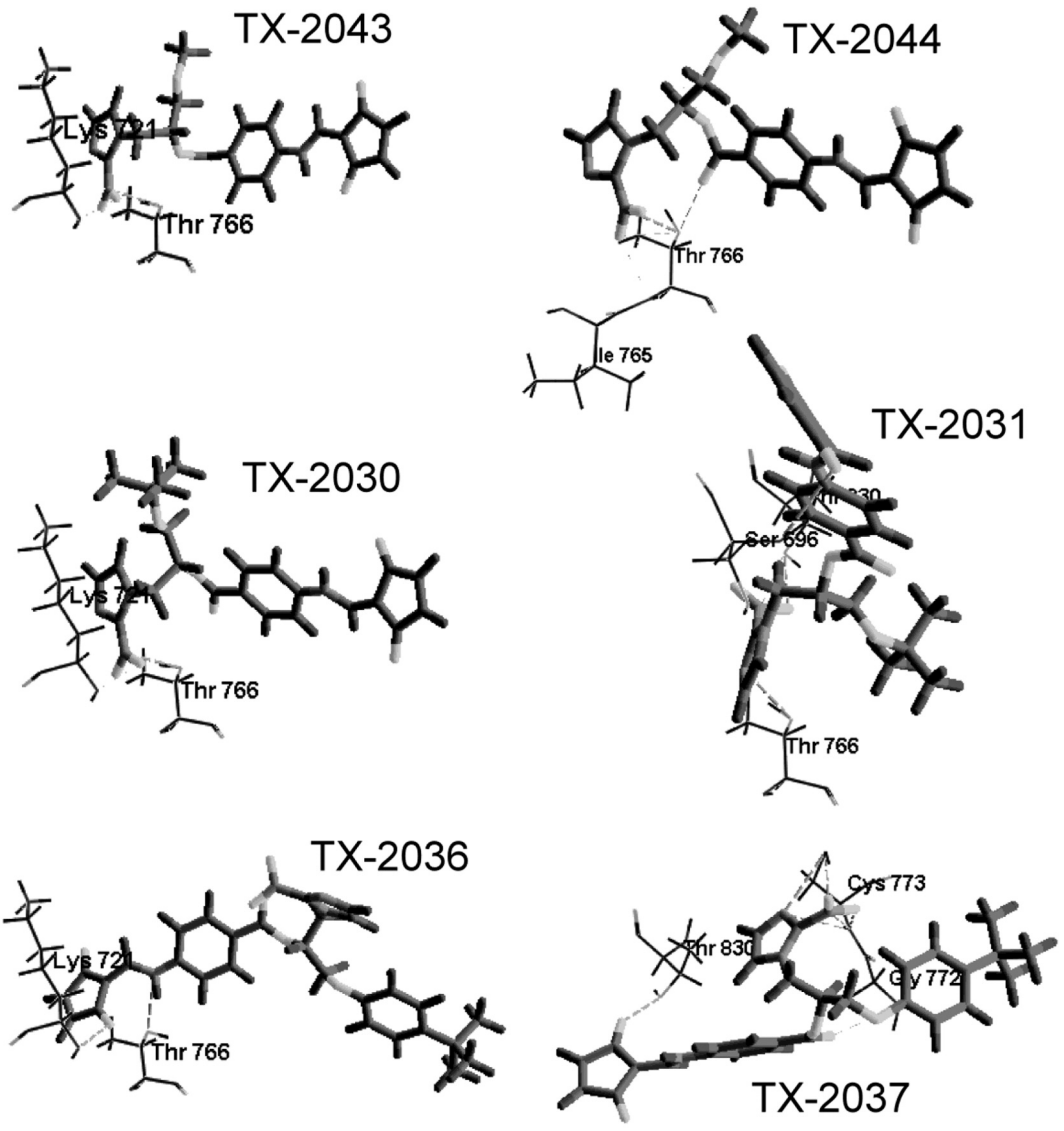

Figure 4. *Interactive profile of TX-2036 derivatives with EGFR-tyk. R-configured TX-2036 derivatives (TX-2043, -2030, -2036) interacted same amino acid residues (Lys^{721}, Thr^{766}). S-configured derivatives reacted with Ile^{765}, Thr^{766} (TX-2044), Ser^{696}, Thr^{766}, Thr^{830} (TX-2031), Gly772, Cys^{773}, Thr^{830} (TX-2037).*

Discussion

TX-2036 possesses an asymmetric carbon and stereoisomers (*R*- and *S*-enantiomer) have been reported. The three-dimensional aspects of TX-2036 derivatives need to be elucidated in order to obtain a clearer understanding of their molecular features. The inhibitory effect of *R*-configured TX-2036 derivatives on EGFR-tyk activity were stronger than those of *S*-configured derivatives. EGFR-tyk inhibition was 10 times different between *R*- and *S*-configured derivatives, and the IC_{50} values of the *R*-, *S*-enantiomers were 1.8-21.3 μM and 18.4-213.0 μM, respectively. The

Table II. *Interactive analysis of TX-2036 derivatives with tyrosine kinase domain.*

TXs (chirality)	Interactive amino acids*
TX-2043 (R)	Lys^{721}, Thr^{766}
TX-2044 (S)	Ile^{765}, Thr^{766}
TX-2030 (R)	Lys^{721}, Thr^{766}
TX-2031 (S)	Ser^{696}, Thr^{766}, Thr^{830}
TX-2036 (R)	Lys^{721}, Thr^{766}
TX-2037 (S)	Gly^{772}, Cys773, Thr^{830}

*Each TX-2036 derivative interacted with indicated amino acid residues of tyrosine kinase domain of EGFR.

optical activity of TX-2036 derivatives appeared to affect EGFR-tyk function. In a molecular interactive simulation, *R*- and *S*-configured TX-2036 derivatives were bindable in the EGFR-tyk. A molecular simulation confirmed that all *R*-configured derivatives (TX-2043, -2030, and -2036) interacted with Lys^{721} and Thr^{766} of the EGFR-tyk. On the other hand, in the *S*-configured derivatives, interaction sites differed from *R*-configured derivatives. The interacting amino acid residues of the EGFR-tyk differed for each *S*-derivative were as follows: TX-2044 (Ile^{765} and Thr^{766}), TX-2031 (Ser^{696}, Thr^{766}, and Thr^{830}), TX-2037 (Gly^{772}, Cys^{773}, and Thr^{830}). No significant differences were observed in the positions at which the *R*- and *S*-derivatives fit into the EGFR-tyk; however, the microenvironment of the interaction differed. By introducing an asymmetric center into the TX-2036 series, it became possible to modify their functions without changing molecular weights.

Based on an analysis using the stereo-hydrophobicity parameter dGW (10, 11), it was confirmed that a molecule with a bulky alkyl chain ((*tert*-butyl)$_2$-C_2H_4: dGW=–0.689kJ/mol) had lower hydrophobicity than that with a linear alkyl chain ($C_{10}H_{22}$: dGW=–0.708kJ/mol), and the degree of hydrophobicity may be adjusted by introducing a bulky region. The absolute value of the difference in dGW value between the $C_{10}H_{22}$-straight alkyl molecule and the (*tert*-butyl)$_2$-C_2H_4 alkyl molecule was 0.019 kJ/mol. This difference was less than that corresponding to the difference of one carbone group (CH_2) obtained from a comparison of the dGW values of the C_{10}-straight alkyl molecule and C_9-straight alkyl molecule, and it was possible to finely adjust the degree of hydrophobicity. Hydrophobicity is one of the factors that influence the ability to interact with pathogenic molecules. It was considered that the hydrophobicity of the designed TX-2036 derivatives could be finely adjusted by tuning the chain length and bulkiness of the introduced alkyl side chain.

The bulkiness of a molecule appears to correlate with free energy, and if it has a bulky structure, the entropy of the molecule is expected to increase. This example had been reported in consideration of Gibbs free energy in the molecular design of other TX-derivatives (*e.g.* haloacetylcarbamoyl-2-nitroimidazole compounds) (2). It is described by the Gibbs free energy (G=U + pV - TS; where G: free energy, U: internal energy, p: pressure, V: volume, T: temperature, S: entropy). Heat formation (total) energy is one of the indices for molecular bulkiness (volume), and the order of these TX-2036 derivatives was *p-tert*-butyl compounds (TX-2036 and -2037: 4.7-18.6 kcal/mol) <methyl compounds (TX-2043 and -2044: 8.8-22.9 kcal/mol) <*tert*-butyl compounds (TX-2030 and -2031: 13.8-27.0 kcal/mol) (4). We considered the molecular design of a *p-tert*-butyl moiety to have a bulky appearance, but to be energetically compact. The introduction of a compactly folded structure in the molecular design appears to promote energy compactness. The balance between various parameters, such as molecular compactness, stereo-hydrophobicity, and reactivity (stability), will be important for the development of efficient kinase (*e.g.* EGFR-tyk) control compounds. In developing an anticancer drug, it is more efficient to use parameters based on dynamic structural information than to search only for biological activity. Thus far, we reported the use of three-dimensional hydrophobic parameter (dGW) and electrostatic potential field (ESP) in molecular design (4, 6, 7, 9, 12). In the present study, we considered the influence of the bulkiness of the structure attached to the pharmacophore through the structural analysis of TX-2036 derivatives. In particular, the *p-tert*-butyl structure appears bulky and is considered useful in the molecular design of anticancer drugs as a component that is energetically stable. We are proceeding with the analysis of the correlation between the kinase inhibition and the anti-cancer activity of the TX-2036 series introduced with the similar structure of *p-tert*-butyl.

Conflicts of Interest

The Authors declare no conflicts of interest regarding this study.

Authors' Contributions

K.O., A.T. and Y.U. carried out the experiment. K.O. wrote the manuscript. H.H. helped supervise the project. All Authors provided critical feedback and helped shape the research, analysis and manuscript.

Acknowledgements

This work was supported, in part, by a Grant-in-Aid for Scientific Research (18K06764) from the Ministry of Education, Culture, Sports, Science and Technology of the Japanese Government.

References

1 Jin CZ, Nagasawa H, Shimamura M, Uto Y, Inayama S, Takeuchi Y, Kirk KL and Hori H: Angiogenesis inhibitor TX-1898: syntheses of the enantiomers of sterically diverse haloacetylcarbamoyl-2-nitroimidazole hypoxic cell radiosensitizers. Bioorg Med Chem *12(18)*: 4917-4927, 2004. PMID: 15336271. DOI: 10.1016/j.bmc.2004.06.039

2 Ohkura K, Uto Y, Nagasawa H and Hori H: Effect of molecular chirality and side chain bulkiness on angiogenesis of haloacetylcarbamoyl-2-nitroimidazole compounds. Anticancer Res *27(6A)*: 3693-3700, 2007. PMID: 17970030.

3 Uto Y, Nagasawa H, Jin CZ, Nakayama S, Tanaka A, Kiyoi S, Nakashima H, Shimamura M, Inayama S, Fujiwara T, Takeuchi Y, Uehara Y, Kirk KL, Nakata E and Hori H: Design of antiangiogenic hypoxic cell radiosensitizers: 2-nitroimidazoles containing a 2-aminomethylene-4-cyclopentene-1,3-dione moiety. Bioorg Med Chem *16(11)*: 6042-6053, 2008. PMID: 18474428. DOI: 10.1016/j.bmc.2008.04.041

4 Ohkura K, Tabata A, Uto Y and Hori H: Correlation between radiosensitizing activity and the stereo-structure of the TX-2036 series of molecules. Anticancer Res *39(8)*: 4479-4483, 2019. PMID: 31366548. DOI: 10.21873/anticanres.13622

5 Murakami Y, Fukazawa H, Mizuno S and Uehara Y: Conversion of epidermal growth factor (EGF) into a stimulatory ligand for A431-cell growth by herbimycin A by decreasing the level of expression of EGF receptor. Biochem J *301*: 57-62, 1994. PMID: 8037691. DOI: 10.1042/bj3010057

6 Ohkura K, Sukeno A, Yamamoto K, Nagamune H, Maeda T and Kourai H: Analysis of structural features of bis-quaternary ammonium antimicrobial agents 4,4'-(alpha,omega-polymethylenedithio)bis(1-alkylpyridinium iodide)s using computational simulation. Bioorg Med Chem *11(23)*: 5035-5043, 2003. PMID: 14604666. DOI: 10.1016/j.bmc.2003.08.027

7 Ohkura K, Sukeno A, Nagamune H and Kourai H: Bridge-linked bis-quaternary ammonium anti-microbial agents: relationship between cytotoxicity and anti-bacterial activity of 5,5'-[2,2'-(tetramethylenedicarbonyldioxy)-diethyl] bis (3-alkyl-4-methylthiazonium iodide)s. Bioorg Med Chem *13(7)*: 2579-2587, 2005. PMID: 15755659. DOI: 10.1016/j.bmc.2005.01.030

8 Ohkura K, Kawaguchi Y, Tatematsu Y, Uto Y and Hori H: An antitumor 2-hydroxyarylidene-4-cyclopentene-1,3-dione as a protein tyrosine kinase inhibitor: Interaction between TX-1123 derivatives and Src kinase. Anticancer Res *36(7)*: 3645-3649, 2016. PMID: 27354635.

9 Ohkura K, Tatematsu Y, Kawaguchi Y, Uto Y and Hori H: Interactive analysis of TX-1123 with cyclo-oxygenase: Design of COX2 selective TX analogs. Anticancer Res *37(7)*: 3849-3854, 2017. PMID: 28668885. DOI: 10.21873/anticanres.11764

10 Ohkura K and Hori H: Analysis of structure-permeability correlation of nitrophenol analogues in newborn rat abdominal skin using semiempirical molecular orbital calculation. Bioorg Med Chem *7(2)*: 309-314, 1999. PMID: 10218822. DOI: 10.1016/s0968-0896(98)00200-4

11 Zhu JW, Nagasawa H, Nagura F, Mohamad SB, Uto Y, Ohkura K and Hori H: Elucidation of strict structural requirements of brefeldin A as an inducer of differentiation and apoptosis. Bioorg Med Chem *8(2)*: 455-463, 2000. PMID: 10722169. DOI: 10.1016/s0968-0896(99)00297-7

12 Kawaguchi Y, Tatematsu Y, Tabata A, Nagamune H and Ohkura K: Cytolytic activity and molecular feature of cardiotoxin and cardiotoxin-like basic protein: The electrostatic potential field is an important factor for cell lytic activity. Anticancer Res *35(8)*: 4515-4519, 2015. PMID: 26168495.

Received May 23, 2020
Revised June 16, 2020
Accepted June 17, 2020